Letter to the Editor

Clinical application of whole-genome sequencing in patients with primary immunodeficiency

To the Editor:

Next-generation sequencing, including whole-exome sequencing and whole-genome sequencing (WES and WGS, respectively), has been successful at identifying causes of Mendelian diseases, even when the condition is seen in a single patient.[1-3] Here, we report our findings from WGS in 6 patients with primary immunodeficiency from 5 families in whom the molecular defect was unknown.

Patients 1 and 2 were full sisters with a history of recurrent infections, including tuberculous lymphadenitis, granulomas, and pneumonias. They had a similarly affected brother. Both patients had an absent rhodamine-based respiratory burst, confirming the diagnosis of chronic granulomatous disease. The parents are distant relatives. Genetic testing was performed at a Clinical Laboratory Improvement Amendments–certified commercial laboratory for *NCF2*, *CYBA*, and *NCF1* and was negative. Of note, the commercial *NCF1* screen examined mutations only in exon 2, which harbors the 2GT deletion that causes most reported cases of *NCF1*-related chronic granulomatous disease.[4] WGS revealed a homozygous 579G>A substitution causing a premature stop codon (Trp193X) in *NCF1* that had previously been reported as causal for chronic granulomatous disease.[5]

Patient 3 was a boy who developed *Pneumocystis jiroveci* pneumonia during the first year of life. There was no family history of primary immunodeficiency. Immune evaluation demonstrated absent serum IgG and IgA. He had normal numbers of B, T, and natural killer (NK) cells by flow cytometry and had normal T-cell proliferative responses to mitogens and antigens. However, the patient lacked any detectable expression of CD40 ligand (CD154) on T cells after stimulation with ionomycin and phorbol myristate acetate, consistent with a diagnosis of X-linked

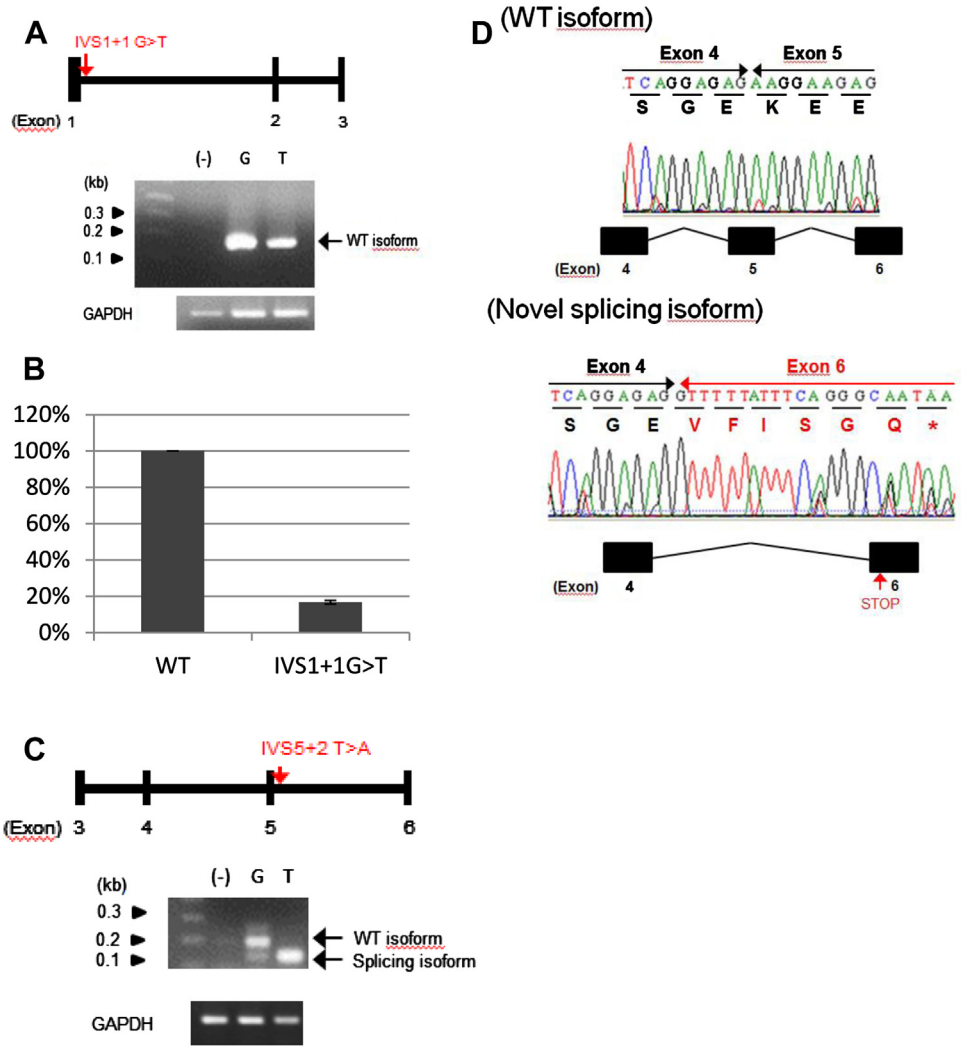

FIG 1. Semi-quantitative PCR and quantitative real-time PCR results of minigene expression. **A,** Minigene-1 (IVS1+1G>T) mRNA expression. **B,** Quantitative Taqman results showing only 16% expression of the WT mRNA in Minigene-1. **C,** Minigene-5 (IVS5+2T>A) mRNA expression. **D,** Sanger sequencing confirmation of IVS5+2T>A, resulting in exon 5 skipping. *GAPDH*, Glyceraldehyde 3-phosphate dehydrogenase.

hyper-IgM syndrome. CD40 ligand gene sequencing was performed at a Clinical Laboratory Improvement Amendments–certified laboratory and no mutations were found, somewhat conflicting with the CD40L expression results. WGS revealed a novel G>T nucleotide substitution in the CD40 ligand gene on the X-chromosome, resulting in a premature stop codon at Glu-230 (Glu230X). Nonsense mutations in neighboring codons (G227X and Q232X) have been previously reported as causes of X-linked hyper-IgM syndrome.[6,7] Based on the mutation's absence in control subjects and in Exome Variant Server (EVS; National Heart, Lung, and Blood Institute GO Exome Sequencing Project, Seattle, Wash; http://evs.gs.washington.edu/EVS/), its predicted functional consequence, and the described disease-causing mutations in neighboring codons, this mutation was judged the likely cause of this patient's immune defect.

Patient 4 was a girl who presented in infancy with a history of failure to thrive and recurrent infections. Flow cytometry showed that she had no T or B cells, but had an elevated percentage of NK cells. T-cell proliferation studies showed no responses to mitogens. A diagnosis of severe combined immunodeficiency (SCID) was made. *RAG1* and *RAG2* genes were sequenced, and no mutations were identified. WGS revealed a homozygous 82-kb deletion spanning exons 1 to 4 in *DCLRE1C* (see Fig E1, *A*, in this article's Online Repository at www.jacionline.org).

Patient 5 was a girl who presented in infancy with failure to thrive and recurrent infections. Immune studies showed absent T cells and B cells and no T-cell proliferative responses to mitogens. All her lymphocytes were NK cells. These findings led to a diagnosis of SCID. Gene sequencing was performed at a Clinical Laboratory Improvement Amendments–certified commercial laboratory for *RAG1*, *RAG2*, and *DCLRE1C*, which are known to be associated with NK-phenotype SCID,[8,9] and the results were negative. WGS revealed a novel heterozygous single nucleotide variant observed at an essential splice site in *DCLRE1C*. This splice site mutation (c.362+2T>A) is absent in controls and in EVS, and is predicted to destroy the canonical splice donor site in intron 5. A splice site variant at the neighboring nucleotide position (c.362+1G>T) is associated with SCID.[9] Further investigation revealed an 82-kb deletion involving exons 1 to 4 in *DCLRE1C* (see Fig E1, *B*). The combined presence of this partial deletion and the c.362+2T>A (IVS5+2T>A) splice site mutation is the likely cause of SCID in this patient.

Patient 6 was a girl whose brother had combined immunodeficiency with a predominance of NK cells. She was investigated immunologically at an early age and had normal T-lymphocyte proliferative responses to mitogens, antigens, and allogeneic cells. She did well clinically until around age 7 years, when she became profoundly lymphopenic and developed very low T-cell function. WGS showed a homozygous essential splice site mutation (c.109+1 G>T) (IVS1+1 G>T) in *DCLRE1C* that was absent in controls. This single nucleotide variant is extremely rare (minor allele frequency = 0.00023 in EVS). This splice site mutation is predicted to destroy the canonical splice donor site in intron 1. However, given the rarity of this variant and the lack of consanguinity in the family, homozygosity was considered unlikely. Deletion screening showed that the patient also had the same 82-kb hemizygous deletion involving exons 1 to 4 of *DCLRE1C* observed in patient 5 (see Fig E1, *C*), which had resulted in miscalling of the single nucleotide variant as homozygous.

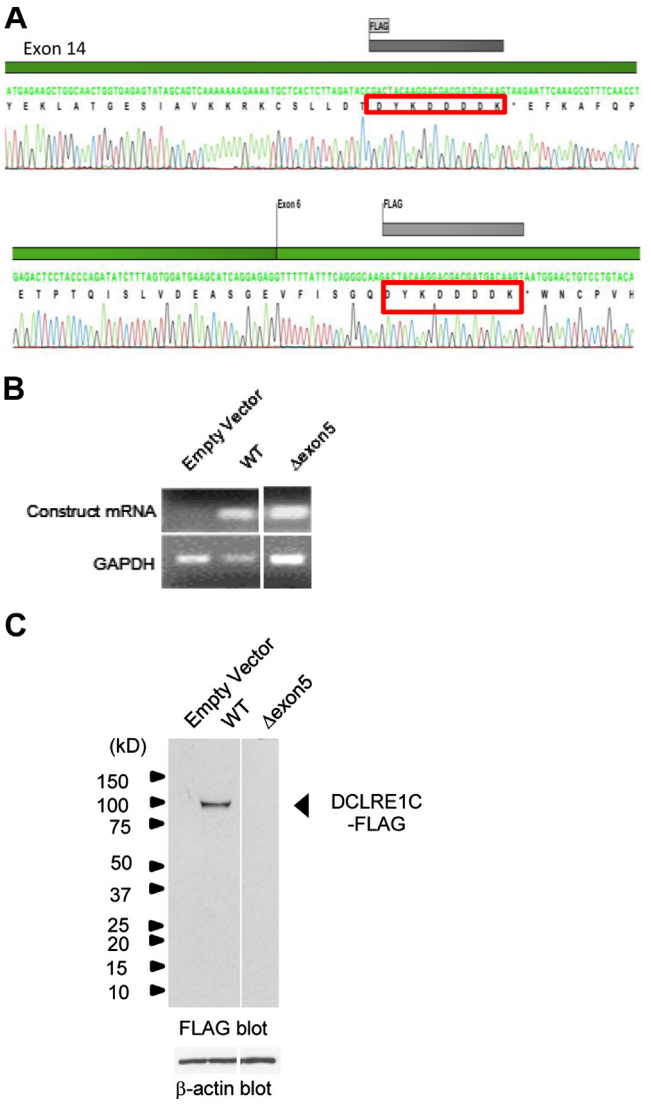

FIG 2. DCLRE1C protein assays. **A,** FLAG-tag insertion in exon 14 of the WT-DCLRE1C construct and exon 6 of the Δexon5 construct. **B,** Semi-quantitative PCR showing the presence of Δexon5 mRNA expression. **C,** Immunoblotting showing the absence of DCLRE1C protein expression in mutant Δexon5 isoform. *GAPDH,* Glyceraldehyde 3-phosphate dehydrogenase.

The difference in disease severity between patients 5 and 6 is interesting because both patients are compound heterozygotes for similar deletion but have different essential splice site mutations. Patient 5 had no T-cell function, while patient 6 had normal T-cell function until around age 7 years. To explain the difference in phenotypic severity, we constructed minigenes for each of the 2 newly identified *DCLRE1C* variants (IVS1+1 G>T and IVS5+2 T>A) (see Fig E2 in this article's Online Repository at www.jacionline.org). A decrease in the wild type DCLRE1C (WT-DCLRE1C) isoform was observed in the IVS1+1 G>T variant construct (Fig 1, *A*). Follow-up quantitative RT-PCR of the wild-type and mutant minigene transcript revealed that the variant produced only 16% of the wild-type transcript (Fig 1, *B*). The IVS5+2 T>A variant construct resulted in a novel isoform in which exon 5 was skipped (Fig 1, *C* and *D*). Both novel

isoforms are predicted to result in abnormal gene and/or protein expression and/or function. We examined the mRNA and protein expression of the full-length WT-DCLRE1C cDNA and the IVS5+2 T>A isoform, in which exon 5 is skipped, using FLAG-tagged constructs (Fig 2, *A*). Although both isoforms showed similar expression at the mRNA level, only the wild-type isoform showed a detectable level of protein (Fig 2, *B* and *C*).

Hence, the IVS1+1 G>T variant found in patient 6 produced some of the canonical wild-type isoform, suggesting that this mutation decreases the splicing efficiency. The IVS5+2 T>A variant from patient 5 did not produce any wild-type isoform, but did produce another isoform. This result is consistent with a model in which patient 6 produced enough wild-type Artemis protein to delay the onset of the patient's combined immunodeficiency, resulting in a less severe phenotype.

The use of next-generation sequencing is accepted for investigating undiagnosed genetic conditions. Here, we show the value of WGS in patients with primary immunodeficiency without identified causal mutations.

We acknowledge the following individuals for the contributions of control samples: Dr William B. Gallentine, Dr Erin L. Heinzen, Dr Aatif M. Husain, Ms Kristen N. Linney, Dr Rodney A. Radtke, Dr Saurabh R. Sinha, Ms Nicole M. Walley, Dr Joseph McEvoy, Dr Anna Need, Mr Jordan Silver, Ms Marlyne Silver, Dr Elizabeth Cirulli, Dr Julie Hoover-Fong, Dr Nara L. Sobreira, Dr David Valle, Dr Robert Brown, Dr Ruth Ottman, Dr Deborah Levy, K. Welsh-Bomer, C. Hulette, J. Burke, Mr David H. Murdock, the MURDOCK Community Registry and Biorepository, Dr Vandana Shashi Ms Kelly Schoch, and Dr Demetre Daskalakis.

We also thank the National Heart, Lung, and Blood Institute GO Exome Sequencing Project and its ongoing studies that produced and provided exome variant calls for comparison: the Lung GO Sequencing Project (HL-102923), the WHI Sequencing Project (HL-102924), the Broad GO Sequencing Project (HL-102925), the Seattle GO Sequencing Project (HL-102926), and the Heart GO Sequencing Project (HL-103010).

Talal Mousallem, MD[a,b]
Thomas J. Urban, PharmD, PhD[c,g]
K. Melodi McSweeney, BS[c,d,h]
Sarah E. Kleinstein, MS[c,d,h]
Mingfu Zhu, PhD[c]
Mehdi Adeli, MD[e]
Roberta E. Parrott, BS[b]
Joseph L. Roberts, MD, PhD[b]
Brian Krueger, PhD[c,h]
Rebecca H. Buckley, MD[b,f]
David B. Goldstein, PhD[c,h]

From [a]the Departments of Internal Medicine and Pediatrics, Wake Forest School of Medicine, Winston Salem, NC; [b]the Department of Pediatrics, Duke University Medical Center, [c]the Center for Human Genome Variation, Duke University School of Medicine, and [d]the Department of Molecular Genetics and Microbiology, Duke University School of Medicine, Durham, NC; [e]Hamad Medical Corporation, Doha, Qatar; [f]the Department of Immunology, Duke University School of Medicine, Durham, NC; [g]Eshelman School of Pharmacy, University of North Carolina, Chapel Hill, NC; and [h]Institute for Genomic Medicine, Columbia University Medical Center, New York, NY. E-mail: tmousall@wakehealth.edu; talal.mousallem@duke.edu. Or: buckl003@mc.duke.edu.

This work was supported by the National Institutes of Health (grants T32 HD43029 and T32 AI7062 provided support for T.M. during his fellowship training at Duke University Medical Center) and a Clinical Immunology Society/Grifols Senior Fellowship Award (to T.M.). The collection of control samples and the production of sequence data were funded in part by the National Institute of Allergy and Infectious Diseases (NIAID) grant UO1AIO67854 (Center for HIV/AIDS Vaccine Immunology ["CHAVI"]).

Disclosure of potential conflict of interest: T. Mousallem has received funding from the Clinical Immunology Society. T. J. Urban is employed by the University of North Carolina at Chapel Hill, which has received or has grants pending from the National Institutes of Health (NIH). B. Krueger has received consultancy fees from LabCorp and Gerson Lehrman Group. R. E. Parrot and R. H. Buckley are employed by the Duke University Medical Center, which has received or has grants pending from Baxter Healthcare and has received funding from the NIH. J. L. Roberts is employed by the Duke University Medical Center and has received compensation for delivering lectures from GlaxoSmithKline. The rest of the authors declare that they have no relevant conflicts of interest.

REFERENCES

1. Worthey EA, Mayer AN, Syverson GD, Helbling D, Bonacci BB, Decker B, et al. Making a definitive diagnosis: successful clinical application of whole exome sequencing in a child with intractable inflammatory bowel disease. Genet Med 2011;13:255-62.
2. Choi M, Scholl UI, Ji W, Liu T, Tikhonova IR, Zumbo P, et al. Genetic diagnosis by whole exome capture and massively parallel DNA sequencing. Proc Natl Acad Sci U S A 2009;106:19096-101.
3. Need AC, Shashi V, Hitomi Y, Schoch K, Shianna KV, McDonald MT, et al. Clinical application of exome sequencing in undiagnosed genetic conditions. J Med Genet 2012;49:353-61.
4. Noack D, Rae J, Cross AR, Ellis BA, Newburger PE, Curnutte JT, et al. Autosomal recessive chronic granulomatous disease caused by defects in NCF-1, the gene encoding the phagocyte p47-phox: mutations not arising in the NCF-1 pseudogenes. Blood 2001;97:305-11.
5. Roos D, de Boer M, Koker MY, Dekker J, Singh-Gupta V, Ahlin A, et al. Chronic granulomatous disease caused by mutations other than the common GT deletion in NCF1, the gene encoding the p47phox component of the phagocyte NADPH oxidase. Hum Mutat 2006;27:1218-29.
6. Lin Q, Rohrer J, Allen RC, Larche M, Greene JM, Shigeoka AO, et al. A single strand conformation polymorphism study of CD40 ligand: efficient mutation analysis and carrier detection for X-linked hyper IgM syndrome. J Clin Invest 1996;97:196-201.
7. Rangel-Santos A, Wakim VL, Jacob CM, Pastorino AC, Cunha JM, Collanieri AC, et al. Molecular characterization of patients with X-linked hyper-IgM syndrome: description of two novel CD40L mutations. Scand J Immunol 2009;69:169-73.
8. Schwarz K, Gauss GH, Ludwig L, Pannicke U, Li Z, Lindner D, et al. RAG mutations in human B cell-negative SCID. Science 1996;274:97-9.
9. Moshous D, Callebaut I, de Chasseval R, Corneo B, Cavazzana-Calvo M, Le Deist F, et al. Artemis, a novel DNA double-strand break repair/V(D)J recombination protein, is mutated in human severe combined immune deficiency. Cell 2001;105:177-86.

http://dx.doi.org/10.1016/j.jaci.2015.02.040

Primary immunodeficiency diseases (PIDs) are highly heterogeneous conditions that would benefit from the application of next-generation sequencing (NGS) in clinical testing. In most cases, PIDs are monogenic and follow simple Mendelian inheritance. However, disease penetrance and expression variability as well as interactions between genetic and environmental factors can contribute to the wide range of phenotypic diversity observed across PIDs.[E1] More than 220 PIDs have been described in the scientific literature to date, and new PIDs continue to be reported.[E2,E3]

Previous attempts to identify the causal mutations underlying PIDs primarily entailed positional cloning or candidate gene sequencing based on known signaling pathways and phenotypic similarity of disease in patients and available murine models. Investigators have also used genome-wide association approaches, which led to the discovery of multiple novel common variable immunodeficiency susceptibility loci.[E4] The use of high-throughput NGS technology has helped explain novel causes of some PIDs. Over the last few years, a number of publications have reported newer molecular defects in PID by NGS technology. Recent examples include the use of whole-exome sequencing (WES) in identifying mutations in *IKBKB* as a cause of combined immunodeficiency (CID), *CSF3R* as a cause of congenital neutropenia, and *CTPS1* associated with defective lymphocyte proliferation and severe EBV infection.[E5-E7]

With the continued discovery of newer molecular defects in PID, keeping up with the growing literature on inherited mutations in PID can be tedious and time consuming. However, several useful online databases are available to researchers. The Human Gene Mutation Database (http://www.hgmd.org) is a comprehensive collection of mutations in nuclear genes that underlie or are associated with human inherited disease. A valuable database for PID is the Resource of Asian Primary Immunodeficiency Disease (http://web16.kazusa.or.jp/rapid/). This is a freely accessible database that contains information on sequence variation, as well as expression at the mRNA and protein levels, in genes reported from patients with PID.

SCID is a fatal PID syndrome characterized by profound deficiencies of T- and B-cell function. It is known to be caused by mutations in at least 13 different genes,[E8,E9] but there are patients with SCID whose mutations remain unknown. Less-severe CID is characterized by impaired but not absent T- and B-cell function. Although some patients with CID have hypomorphic mutations in known SCID-associated genes, the causal mutations for many patients with CID remain elusive. Similarly, although causative mutations for hyper-IgM syndrome have been found in 5 genes,[E10,E11] many patients still lack identification of the causal gene mutation. Chronic granulomatous disease (CGD) is caused by mutations in 5 nicotinamide adenine dinucleotide phosphate oxidase structural genes (*CYBB*, *CYBA*, *NCF1*, *NCF2*, and *NCF4*).[E12] Mutations in *CYBB* (gp91phox) cause X-linked CGD and account for nearly two thirds of the cases. All other described CGD cases have an autosomal-recessive pattern of inheritance.

METHODS

All patients were followed at the Immune Deficiency Foundation's Duke University Primary Immunodeficiency Center of Excellence. All studies were performed with the approval of the Duke University Medical Center's Institutional Review Board and with the written informed consent of the patients or their parents.

WGS

WGS was accomplished using paired-end sequencing on the Illumina HiSeq2000 with average coverage of 39.5 ± 5.8 (range, 33.6-50.0). Reads were aligned to the Human Reference Genome (NCBI36) using BWA software.[E13] Single nucleotide variants (SNVs) and insertions/deletions (INDELs) were called and genotypes assigned using SAMtools.[E14] Control samples (n > 160) were sequenced contemporaneously in the same laboratory, and variants were called and annotated in a manner similar to the patient genomes.

Identification of likely causal variants

The WGS screens were designed to interrogate highly penetrant genotypes that might account for each patient's PID. Patients were screened for putatively functional rare variants that were absent in a cohort of more than 160 unrelated control subjects and were absent or at very low frequencies in the EVS (National Heart, Lung, and Blood Institute GO Exome Sequencing Project; http://evs.gs.washington.edu/EVS/) public database. High-quality variants were annotated using the Sequence Variant Analyzer (http://www.svaproject.org/).[E15] Standard filtering criteria were applied (SNV quality, SNV consensus score, INDEL consensus score of ≥20, INDEL quality ≥ 50, number of reads supporting SNV or INDEL ≥3). Because variants with known or predicted functional consequences are more likely to be causal of such deleterious phenotypes, only functional variants were further considered: missense and nonsense SNVs, stop loss SNVs, frameshift INDELs, and splice site mutations, or structural variants that overlapped genes. Functional variants present in the proband were prioritized as potentially causal as follows: (1) a homozygous (including hemizygous X variants) genotype lacking homozygosity in controls (recessive and X-linked variants) (minor allele frequency < 0.02) and (2) a compound heterozygous (minor allele frequency < 0.03 for each participating variant) genotype that was not observed together in any controls. Known PID genes were included in the initial evaluation of candidate variants lists generated from these tests. Candidate variants were then further prioritized by gene ontology, with higher weight given to variants in genes with a known role in immune function or known expression in relevant cell types. When no interesting genes were identified by these criteria, heterozygous genotypes in patients with very low frequencies in controls (minor allele frequency < 0.02) were also included. This served as an indirect screen for compound heterozygosity that could have been missed on our initial screen, either because of low coverage of 1 of the 2 causal mutations or because 1 of the 2 causal variants was a copy number variant (CNV).

Identification of structural variation

Structural variations (including INDELs, deletions, duplications, and CNVs) were identified using ERDS (Estimation by Read Depth with SNVs, version 1.06; http://www.utahresearch.org/mingfuzhu/erds/) software.[E16] ERDS primarily uses a paired Hidden Markov Model to analyze high-coverage WGS data combining read depth, paired-end, polymorphism, and structural variant signature information with GC corrections. CNVs were detected with default ERDS parameters.[E16]

DCLRE1C splicing studies

Plasmids. Each human *DCLRE1C* exon, including approximately 300 bp of flanking intronic sequence, was amplified from genomic DNA derived from PBMCs of healthy volunteers using PrimeSTAR GXL DNA Polymerase (Takara, Otsu Shiga, Japan). *DCLRE1C* exons were subcloned into the pCR-Blunt II-TOPO vector (Life Technologies, Grand Island, NY) and sequenced. Using pCR-Blunt II-Exon1 and pCR-Blunt II-*DCLRE1C*-Exon5 as templates, the IVS1+1 G>T and IVS5+2 T>A mutants (c.109+1G>T and c.362+2T>A, respectively) were made by PCR-directed mutagenesis using PfuUltra II Fusion HS DNA Polymerase. The products were phosphorylated by T4 polynucleotide kinase (New England Biolabs, Ipswich, Mass), self-ligated using T4 DNA ligase (Promega, Madison, Wis), and

sequenced. Genomic DNAs encoding exons 1 to 3 and exons 3 to 6 were subcloned into pcDNA3.1(+) vector, generating the Minigene-1 and Minigene-5 wild-type (WT) and mutant constructs, respectively.

The 5′ and 3′ ends of the human *DCLRE1C* cDNA sequence were amplified with PrimeSTAR GXL DNA Polymerase. These were subcloned into the pCR-Blunt II-TOPO vector and subjected to sequence analysis (pCR-Blunt II-*DCLRE1C*-A-WT and pCR-Blunt II-*DCLRE1C*-B-WT). Using pCR-Blunt II-*DCLRE1C*-A-WT, the Δexon5 isoform of *DCLRE1C* was made by PCR-directed mutagenesis to remove exon 5 as described above. A FLAG-tag was also added to each isoform by PCR-directed mutagenesis. FLAG-tagged full-length cDNAs encoding *DCLRE1C* were subcloned into pcDNA3.1(+) vector, creating pcDNA3.1(+)-*DCLRE1C*-WT-FLAG and pcDNA3.1(+)-*DCLRE1C*-Δexon5-FLAG constructs.

Minigene assays. Empty pcDNA3.1(+) vector, Minigene-1WT, Minigene-1mutant, Minigene-5WT, and Minigene-5mutant were transfected into COS-7 using Lipofectamine 2000 according to standard protocol. Total RNA was extracted from transfectants after 24 hours, and first-strand cDNA encoding the human *DCLRE1C* minigene was synthesized. DCLRE1C minigene transcript expression levels were detected by semi-quantitative RT-PCR and sequenced. The transcripts of Minigene-1WT and Minigene-1mutant were also detected by quantitative RT-PCR using Taqman one-step PCR Master Mix (Life Technologies) (for primer list, see Table E1).

Immunoblotting. Empty pcDNA3.1 (+) vector, pcDNA3.1(+)-*DCLRE1C*-WT-FLAG, or pcDNA3.1(+)-*DCLRE1C*-Δexon5-FLAG were transfected into COS-7 cells. Cells were lysed with a solution of RIPA Buffer (Sigma-Aldrich, St Louis, Mo), 1 × 0.5 mol/L EDTA, and 1× protease inhibitor (ThermoScientific, Somerset, NJ) 48 hours after transfection. Lysates were subjected to SDS-PAGE gel and transferred to a polyvinylidene difluoride membrane (Millipore, Billerica, Mass). The membranes were incubated with anti-FLAG antibody (1:2000; Sigma-Aldrich) or anti–β-actin (1:10,000; Cell Signalling Technology, Danvers, Mass). Proteins were visualized with the ECL Plus Western Blotting Detection System (GE Healthcare, South Plainfield, NJ).

Verification of variants and communication of results to families

All families underwent genetic counseling at our immunology clinic at the time of participation. The identified variants were confirmed in a Clinical Laboratory Improvement Amendments (CLIA)-certified laboratory before communication to the families.

DISCUSSION

To date, we have performed WGS on 12 primary immunodeficiency disease cases. We identified the causal mutation in 6 (discussed here). Hence, we had a success rate of 50% in identifying the disease-causing mutation.

The use of NGS is accepted for investigating undiagnosed genetic conditions. NGS adds considerable value through its ability to both identify novel and rare mutations in known genes and investigate a broader range of genes than by targeted gene testing.

Commercial laboratories are limited by the nature and cost of targeted gene testing, and sometimes only those gene regions that harbor most of the previously identified mutations are screened. For patients 1 and 2, the causal mutation in exon 7 of *NCF1* was missed by targeted gene testing because the commercial *NCF1* screen examined mutations only in exon 2, which harbors the 2GT deletion that causes most reported cases of *NCF1*-related CGD.[E17] It remains unclear why the nonsense mutation in CD40 ligand gene we identified in patient 3 was missed by the CLIA-certified laboratory. Of note, measurement of CD40L function by assessing the binding of CD40L to the soluble receptor CD40-muIg is available as a clinical test.

Patient 4 was initially screened for mutations only in *RAG1* and *RAG2*, the only known causes of NK-phenotype SCID at the time of her diagnosis.[E18] The Artemis encoding *DCLRE1C* gene was subsequently also found to cause NK-phenotype SCID.[E19] Hypomorphic *DCLRE1C* mutations have also been reported as a cause of partial T- and B-lymphocyte immunodeficiency.[E20] The *DCLRE1C* gene is prone to deletions involving 1 or more of its 14 exons.[E21] One study analyzing *DCLRE1C* mutations in patients with SCID found that 60% of the alleles had a large deletion, mostly involving exons 1 to 3.[E22] Patient 4 in our study was found to be homozygous for the 82-kb deletion involving exons 1 to 4 in *DCLRE1C* (Fig E1, *A*).

The defect in patient 5 was also missed by a CLIA-certified laboratory when she was tested for *DCLRE1C* mutations because targeted gene testing at that time lacked the ability to identify gross deletions and was able to discern only nondiagnostic heterozygosity. Patient 6 was the only patient initially screened via WGS. It is worth noting that even if patient 6 had undergone full SCID candidate gene testing (at significant expense), the cause may have been missed unless an exon array or a multiplex ligation-dependent probe amplification was performed to determine the copy number of the *DCLRE1C* gene, as with patient 5.

Defects involving *DCLRE1C* gross deletions, as we observed in patients 4 to 6, would likely have been missed by targeted gene testing technology, generating ambiguous results because of PCR failure in Sanger sequencing. Even WES may have missed this causal mutation because inferring CNVs is much more challenging and less reliable with exome data.[E23]

The cost of clinical genetic testing in these patients is important to address. For patients 1 and 2, the cost for testing *NCF1*, *NCF2*, and *CYBA* at a CLIA-certified commercial laboratory was $3200 per patient.

Of note, the current cost of sequencing in our research laboratory is around $3200 for WGS and $650 for WES. The current standard turnaround time for WES and WGS at the Duke Center for Human Genome Variation (research laboratory) is 49 days. For urgent cases, rapid sequencing can be done at the Duke Center for Human Genome Variation in about 2 weeks. Standard turnaround time will vary by research or clinical laboratory. Interestingly, a group reported a system that permits WGS with bioinformatics analysis of suspected genetic disorders within 50 hours. This time frame is very promising for emergency use when rapid diagnosis is needed in an emergency or critical care setting.[E24]

NGS panels for a selected group of genes have become commercially available and are proving to be more popular and economical than sequencing individual genes. One recent report suggests that NGS-based evaluation may be used as a first-line genetic test for cases of PID.[E25] Furthermore, NGS may be clinically and economically beneficial in patients who remain undiagnosed despite traditional genetic diagnostic evaluations.[E26]

NGS has been clearly shown to be a successful approach in identifying causes of Mendelian diseases, even when the condition is seen in a single patient. Variations in data generation across platforms and methods of data interpretation can be challenging in this context, particularly when disease-causing variation is very rare and present in only a single family. However, a set of criteria has recently been proposed for deciding whether

the clinical and experimental data are sufficient to establish a causal relationship with only 1 affected individual.[E27] There are challenges associated with NGS technology, including the complexity of data analysis and the potential for the mapping and variant calling algorithms to miss variants. Reliability of NGS data analysis is highly dependent on the choice of a reliable control cohort of high quality and depth. In addition, this technology requires extensive interplay between geneticists, clinicians, and bioinformaticians and the analysis can be very complex.

It is also likely that a small proportion of the genome will remain refractory to NGS. WES and WGS offer the advantage of interrogating the entire genome, rather than being limited to only likely gene candidates, and WGS may prove to be faster and less expensive than targeted gene approaches in many cases.

Although the patients studied already had a clinical diagnosis, determining the underlying genetic causes of their diseases is important for several reasons. First, it may have an impact on clinical care. For example, patients with Artemis deficiency are at an increased risk for deleterious effects from ionizing radiation. In addition, we have found that patients and families lacking a definitive genetic diagnosis have emotional distress from lack of information regarding genetic counseling and uncertainty regarding potential future impact on subsequent pregnancies.

The choice between performing WGS or WES is not an easy one. WES is less expensive and more readily available, but can miss disease-causing mutations in noncoding regions. Examples include intronic *GATA2* mutations in patients with MonoMAC syndrome[E28] and a mutation in the 5′ untranslated region of *IKBKG* (nuclear factor-kappaB essential modifier) in X-linked ectodermal dysplasia with immunodeficiency.[E29] Identification of large structural variations such as deletions was formerly problematic with WES. However, recent new analytical approaches make it possible to screen for clinically relevant CNVs using existing exome-based CNV detection methods.[E30] Yet, WGS is known to provide more accurate inference about structural variation than WES.

In summary, this work suggests that the application of NGS should be strongly considered in all PID cases in whom the initial studies have not determined the molecular etiology of disease.

REFERENCES

E1. Notarangelo LD. Primary immunodeficiencies. J Allergy Clin Immunol 2010; 125:S182-94.
E2. Parvaneh N, Casanova JL, Notarangelo LD, Conley ME. Primary immunodeficiencies: a rapidly evolving story. J Allergy Clin Immunol 2013;131:314-23.
E3. Al-Herz W, Bousfiha A, Casanova JL, Chatila T, Conley ME, Cunningham-Rundles C, et al. Primary immunodeficiency diseases: an update on the classification from the International Union of Immunological Societies Expert Committee for Primary Immunodeficiency. Front Immunol 2014;5:162.
E4. Orange JS, Glessner JT, Resnick E, Sullivan KE, Lucas M, Ferry B, et al. Genome-wide association identifies diverse causes of common variable immunodeficiency. J Allergy Clin Immunol 2011;127:1360-7.e6.
E5. Triot A, Järvinen PM, Arostegui JI, Murugan D, Kohistani N, Dapena Díaz JL, et al. Inherited biallelic CSF3R mutations in severe congenital neutropenia. Blood 2014;123:3811-7.
E6. Mousallem T, Yang J, Urban T, Wang H, Adeli M, Parrott RE, et al. A nonsense mutation in IKBKB causes combined immunodeficiency. Blood 2014;124: 2046-50.
E7. Martin E, Palmic N, Sanquer S, Lenoir C, Hauck F, Mongellaz C, et al. CTP synthase 1 deficiency in humans reveals its central role in lymphocyte proliferation. Nature 2014;510:288-92.
E8. Buckley RH. Transplantation of hematopoietic stem cells in human severe combined immunodeficiency: long-term outcomes. Immunol Res 2011;49:25-43.
E9. Pannicke U, Honig M, Hess I, Friesen C, Holzmann K, Rump EM, et al. Reticular dysgenesis (aleukocytosis) is caused by mutations in the gene encoding mitochondrial adenylate kinase 2. Nat Genet 2009;41:101-5.
E10. Durandy A, Taubenheim N, Peron S, Fischer A. Pathophysiology of B-cell intrinsic immunoglobulin class switch recombination deficiencies. Adv Immunol 2007;94:275-306.
E11. Kracker S, Gardes P, Durandy A. Inherited defects of immunoglobulin class switch recombination. Adv Exp Med Biol 2010;685:166-74.
E12. Matute JD, Arias AA, Wright NA, Wrobel I, Waterhouse CC, Li XJ, et al. A new genetic subgroup of chronic granulomatous disease with autosomal recessive mutations in p40 phox and selective defects in neutrophil NADPH oxidase activity. Blood 2009;114:3309-15.
E13. Li H, Durbin R. Fast and accurate short read alignment with Burrows-Wheeler transform. Bioinformatics 2009;25:1754-60.
E14. Li H, Handsaker B, Wysoker A, Fennell T, Ruan J, Homer N, et al. The Sequence Alignment/Map format and SAMtools. Bioinformatics 2009;25:2078-9.
E15. Ge D, Ruzzo EK, Shianna KV, He M, Pelak K, Heinzen EL, et al. SVA: software for annotating and visualizing sequenced human genomes. Bioinformatics 2011; 27:1998-2000.
E16. Zhu M, Need AC, Han Y, Ge D, Maia JM, Zhu Q, et al. Using ERDS to infer copy-number variants in high-coverage genomes. Am J Hum Genet 2012;91: 408-21.
E17. Noack D, Rae J, Cross AR, Ellis BA, Newburger PE, Curnutte JT, et al. Autosomal recessive chronic granulomatous disease caused by defects in NCF-1, the gene encoding the phagocyte p47-phox: mutations not arising in the NCF-1 pseudogenes. Blood 2001;97:305-11.
E18. Schwarz K, Gauss GH, Ludwig L, Pannicke U, Li Z, Lindner D, et al. RAG mutations in human B cell-negative SCID. Science 1996;274:97-9.
E19. Moshous D, Callebaut I, de Chasseval R, Corneo B, Cavazzana-Calvo M, Le Deist F, et al. Artemis, a novel DNA double-strand break repair/V(D)J recombination protein, is mutated in human severe combined immune deficiency. Cell 2001;105:177-86.
E20. Moshous D, Pannetier C, de Chasseval R, le Deist F, Cavazzana-Calvo M, Romana S, et al. Partial T and B lymphocyte immunodeficiency and predisposition to lymphoma in patients with hypomorphic mutations in Artemis. J Clin Invest 2003;111:381-7.
E21. van Zelm MC, Geertsema C, Nieuwenhuis N, de Ridder D, Conley ME, Schiff C, et al. Gross deletions involving IGHM, BTK, or Artemis: a model for genomic lesions mediated by transposable elements. Am J Hum Genet 2008;82:320-32.
E22. Pannicke U, Honig M, Schulze I, Rohr J, Heinz GA, Braun S, et al. The most frequent DCLRE1C (ARTEMIS) mutations are based on homologous recombination events. Hum Mutat 2010;31:197-207.
E23. Fromer M, Moran JL, Chambert K, Banks E, Bergen SE, Ruderfer DM, et al. Discovery and statistical genotyping of copy-number variation from whole-exome sequencing depth. Am J Hum Genet 2012;91:597-607.
E24. Saunders CJ, Miller NA, Soden SE, Dinwiddie DL, Noll A, Alnadi NA, et al. Rapid whole-genome sequencing for genetic disease diagnosis in neonatal intensive care units. Sci Transl Med 2012;4:154ra135.
E25. Nijman IJ, van Montfrans JM, Hoogstraat M, Boes ML, van de Corput L, Renner ED, et al. Targeted next-generation sequencing: a novel diagnostic tool for primary immunodeficiencies. J Allergy Clin Immunol 2014;133: 529-34.
E26. Shashi V, McConkie-Rosell A, Rosell B, Schoch K, Vellore K, McDonald M, et al. The utility of the traditional medical genetics diagnostic evaluation in the context of next-generation sequencing for undiagnosed genetic disorders. Genet Med 2014;16:176-82.
E27. Casanova JL, Conley ME, Seligman SJ, L4 Abel, Notarangelo LD. Guidelines for genetic studies in single patients: lessons from primary immunodeficiencies. J Exp Med 2014;211:2137-49.
E28. Hsu AP, Johnson KD, Falcone EL, Sanalkumar R, Sanchez L, Hickstein DD, et al. GATA2 haploinsufficiency caused by mutations in a conserved intronic element leads to MonoMAC syndrome. Blood 2013;121:3830-7, S1-7.
E29. Mooster JL, Cancrini C, Simonetti A, Rossi P, Di Matteo G, Romiti ML, et al. Immune deficiency caused by impaired expression of nuclear factor-kappaB essential modifier (NEMO) because of a mutation in the 5′ untranslated region of the NEMO gene. J Allergy Clin Immunol 2010;126:127-32.e7.
E30. Kadalayil L, Rafiq S, Rose-Zerilli MJ, Pengelly RJ, Parker H, Oscier D, et al. Exome sequence read depth methods for identifying copy number changes. Brief Bioinform August 28, 2014 [Epub ahead of print].

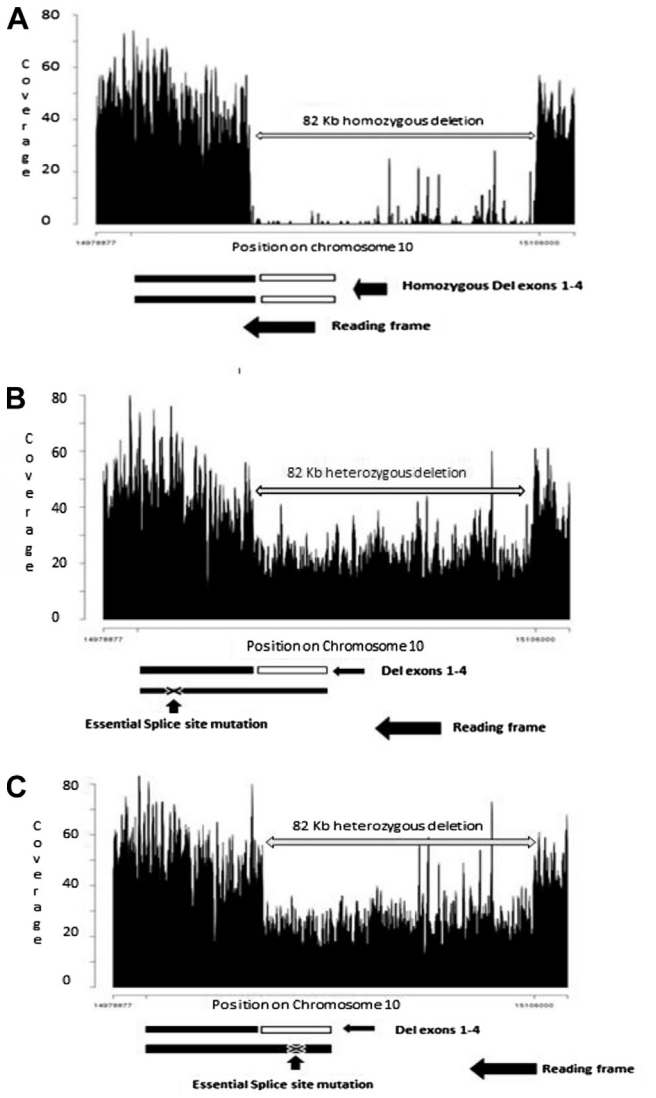

FIG E1. Detection of CNVs by ERDS. A read depth (RD) of 40 indicates that both copies of the gene are present; an RD of 20 suggests that 1 gene copy is missing; an RD of 0 suggests that both gene copies are missing. Detection of 82-kb deletion on chromosome 10 including exons 1 to 4 of *DCLRE1C* in patients 4 **(A)**, 5 **(B)**, and 6 **(C)**. The deletion is homozygous in patient 4.

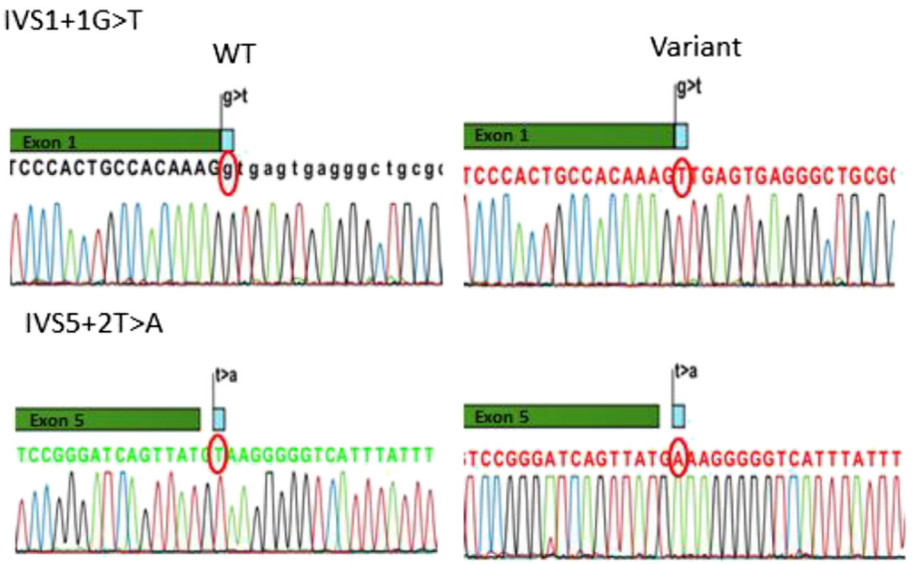

FIG E2. Sanger confirmation of IVS1+G>T and IVS5+2T>A *DCLRE1C* variant constructs.

TABLE E1. Primer list

	Primer	Sequence (5′-3′)	Restriction site incorporated
Plasmid construction and sequencing			
Minigene 1	DCLRE1C-Exon1-F	GCTAGCTTGGCTTCAGCTGCGGTTTT	NheI
	DCLRE1C-Exon1-R	CTTAAGCACCAGCAAAGCTACCAAGA	AflII
	DCLRE1C-Exon2-F	CTTAAGTCTCATTCTTCTGTGGCTGC	AflII
	DCLRE1C-Exon2-R	AAGCTTCAAGTTCACAAACAGCCAAAGC	HindIII
	DCLRE1C-Exon3A-F	AAGCTTGCTCTTGGTGGCACTGAAAT	HindIII
	DCLRE1C-Exon3A-R	CTCGAGTTCGTTTCTTCCAAAATCTGTATTTCG	XhoI
Minigene 5	DCLRE1C-Exon3B-F	GCTAGCCTGTTCACCTGTGACTAAGG	NheI
	DCLRE1C-Exon3B-R	CTTAAGTACAAGTGTGTGCCACGACA	AflII
	DCLRE1C-Exon4-F	CTTAAGCATGGAAACAGAATTGTGTCAGAG	AflII
	DCLRE1C-Exon4-R	AAGCTTGTAGTTTTGTGAGTCCAGCC	HindIII
	DCLRE1C-Exon5-F	AAGCTTTGTGAACAGTCAGGCACACA	HindIII
	DCLRE1C-Exon5-R	GGATCCAAACTCACTGCAGCCTCCAA	BamHI
	DCLRE1C-Exon6-F	GGATCCCAAACTGGGTAGCATCTCCA	BamHI
	DCLRE1C-Exon6-R	CTCGAGTCACCTGAAGTCAGGAGTTC	XhoI
WT-DCLRE1C	DCLRE1C-cDNA-A-F	CTTAAGTTGGCTTCAGCTGCGGTTTT	NheI
	DCLRE1C-cDNA-A-R	TGCTCCTTTCTCCAAACCAC	
	DCLRE1C-cDNA-B-F	AGGAGTCCAGGTTCATGTGA	
	DCLRE1C-cDNA-B-R	CTCGAGGTTGCTCTAGGTTGAAACGC	XhoI
Mutagenesis of Minigene 1 and Minigene 5			
	DCLRE1C-IVS1-mutagenesis-F	TTGAGTGAGGGCTGCG	
	DCLRE1C-IVS1-mutagenesis-R	CTTTGTGGCAGTGGGACA	
	DCLRE1C-IVS5-mutagenesis-F	GAAAGGGGGTCATTTATTTTGTCATTT	
	DCLRE1C-IVS5-mutagenesis-R	ATAACTGATCCCGGACAGTG	
FLAG introduction			
	DCLRE1C-WT-FLAG-F1	GACAAGTAAGAATTCAAAGCGTTTCAACCT	
	DCLRE1C-WT-FLAG-R1	GTAGTCGGTATCTAAGAGTGAGCATT	
	DCLRE1C-WT-FLAG-F2	GACGATGACAAGTAAGAATTCAAAGCGTTT	
	DCLRE1C-WT-FLAG-R2	GTCCTTGTAGTCGGTATCTAAGAGT	
	DCLRE1C-IVS1-FLAG-F1	GACAAGTGAGGGCTGCGCGT	
	DCLRE1C-IVS1-FLAG-R1	GTAGTCCTCAACTTTGTGGCAGTG	
	DCLRE1C-IVS1-FLAG-F2	GACGATGACAAGTGAGGGCTG	
	DCLRE1C-IVS1-FLAG-R2	GTCCTTGTAGTCCTCAACTTTGTGG	
	DCLRE1C-IVS5-FLAG-F1	GACAAGTAATGGAACTGTCCTGTACAC	
	DCLRE1C-IVS5-FLAG-R1	GTAGTCTTGCCCTGAAATAAAAACCTCTC	
	DCLRE1C-IVS5-FLAG-F2	GACGATGACAAGTAATGGAACTGTCCT	
	DCLRE1C-IVS5-FLAG-R2	GTCCTTGTAGTCTTGCCCTGAAATAAAAAC	
RT-PCR primers			
Control	GAPDH-F	ACCACAGTCCATGCCATCA	
	GAPDH-R	CACCACCCTGTTGCTGTAGCC	
Minigene 1	DCLRE1C-Exon1-F	GCTAGCTTGGCTTCAGCTGCGGTTTT	
	DCLRE1C-Exon3A-R	CTCGAGTTCGTTTCTTCCAAAATCTGTATTTCG	
Minigene 5	DCLRE1C-Exon4F2	ATCGAGACTCCTACCCAGAT	
	DCLRE1C-Exon6R2	GAGTGCAGAAGCTCCATTCT	
FLAG constructs	IVS-cDNA-RT-F	CAGCTGCGGTTTGGGGTCC	
	IVS1-muta-R	CTTTGTGGCAGTGGGACA	

F, Forward primer; *GAPDH*, glyceraldehyde 3-phosphate dehydrogenase; *R*, reverse primer.